XLI CILAMCE
XLI Ibero-Latin American Congress on Computational Methods in Engineering
16-19 November, 2020 FOZ DO IGUAÇU PARANÁ - BRAZIL

CFD APPLIED TO THE SIMULATIONS OF THE ANGLE OF ATTACK AND FLUTTER DERIVATIVES OF AN AIRFOIL NACA0012

Lucas Lucinda de Sá[1], Patrícia Habib Hallak[1],

[1]*Post Graduate Program in Civil Engineering, Universidade Federal de Juiz de Fora*
Faculdade de Engenharia, Rua José Lourenço Kelmer, São Pedro, 36036-900, Juiz de Fora - MG, Brasil
lucas.lucinda@engenharia.ufjf.br, patricia.hallak@ufjf.edu.br

Abstract.

This paper presents a study of the aerodynamic behavior of a NACA0012 airfoil modeled in two dimensions using computational fluid dynamics. In the first analysis, the aerodynamic lift and drag coefficients were obtained for a range of angles of attack for Reynolds number equal to 700000. The kωSST turbulence model was employed, and the model has no displacement. The second analysis lies in the identification of the flutter derivatives in motion-related fluid forces exerted on an airfoil, with Reynolds number equal to 800. The methodology is based on the idea proposed by Le Maıtre et al. [1], which assumes a linear relationship between force functions and the laws of motion of the airfoil so that superposition in both frequency and freedom spaces is allowed. To obtain the flutter derivatives a known sinusoidal vibrations were applied in the airfoil mid-chord. With the response of these coefficients and using Fourier transforms for the treatment of their signals, the flutter derivatives are subsequently calculated. A numerical model to solve the incompressible Navier-Stokes equations is proposed using the OpenFOAM CFD free code. The results from both sets of the simulation were compared with those from the literature, validating the numerical models.

Keywords: Airfoil, Flutter derivatives, Computational fluid dynamics, OpenFOAM, Angle of attack, k ωSST

1 Introduction

Airfoil profiles are essential for several industrial areas. Consequently, more and more studies on fluid dynamics are used to analyze this type of geometry and its interactions with the flow.

Some phenomena resulting from fluid-structure contact have become targets of studies in different works in the last 100 years. In this work, two different situations stand out. The first refers to the variation of the aerodynamic coefficients with the variation of the angle of attack, in a static and turbulent condition. From a certain angle, the flow takes off from the airfoil surface, the drag increases sharply while the lift decreases, characterizing an aerodynamic phenomenon called stall.

Another phenomenon worth mentioning is flutter, a class of aeroelastic phenomenon associated with divergent oscillatory movement identified by the coupling of two degrees of freedom of the structure, that of rotation (torsion) and that of vertical motion (flexion). It is a phenomenon observed in structures such as bridges or airplane wings (Blevins, 2001)[2]. Dowell et al. [3] describes the phenomenon of flutter like the most worrying, as it causes an instability that can damage and induce the structure to fail.

This paper has as main objective the study of these phenomena in a NACA 0012. For this purpose the computational fluid dynamics (CFD - *computational fluid dynamic*) and the open-source OpenFOAM was used. This research seeks: to validate the methodology used in CFD for the static analysis of a 2D airfoil at different angles of attack, submitted to an incompressible and turbulent flow; to verify the choice of mesh and the algorithm that imposes movement of the mesh and the body; to obtain the flutter derivatives for the airfoil under a laminar and incompressible regime.

After this introduction, the relevant theories and the numerical techniques used are presented next. Examples, results, and discussions are presented in Section 3. Finally, there are the conclusions and future work.

2 Theoretical basis

2.1 Governing equations in fluid dynamics

The physical and mathematical model uses the Navier Stokes equations of conservation of mass and momentum for incompressible and viscous flows.

$$\nabla.\vec{v} = 0, \tag{1}$$

$$\rho\frac{\partial\vec{v}}{\partial t} + \rho\nabla.\vec{v}\vec{v} = -\nabla.p + \nabla.(\bar{\bar{\tau}}) + \rho\vec{g} + \vec{F}. \tag{2}$$

These equations make it possible to determine the velocity and pressure field of the fluid, with ρ being the density of the fluid, p the pressure, $\vec{v}$ the velocity field, $\bar{\bar{\tau}} = \mu\left[\left(\nabla\vec{v} + \nabla\vec{v}^T\right)\right]$ is the tensor viscous part, μ is viscosity, $\rho\vec{g}$ and $\vec{F}$ are gravitational and external forces, respectively.

The $k-\omega$ SST [4] turbulence model combined with logarithmic wall functions is used. It consists of the solution of two differential equations, one for the kinetic energy k and another for the specific dissipation rate of the turbulence ω. The term SST is an acronym for *shear stress transport*. For isotropic turbulence, the initial values of the kinetic energy of the turbulence and the dissipation rate can be estimated by eq. (3) [5].

$$k = \frac{3}{2}(IU_\infty)^2, \qquad \omega = \frac{k^{0,5}}{C_\mu^{0,25}L}, \tag{3}$$

where U_{inf} is the freestream velocity, I is the turbulence intensity, L is a characteristic length, and C_μ is an empirical constant equal to 0.09.

2.2 Flutter equations

The formulation proposed by Scanlan and Tomko [6] is used. This formulation connects the aerodynamic forces exerted by the forced movement in a 2D airfoil with the flutter parameters. Linearity is assumed between the force and moment functions with the airfoil motion. Therefore, for small oscillations and a uniform velocity U_∞ the expressions proposed by Scanlan and Tomko [6] are:

$$L = \frac{\rho U_\infty^2(2b)}{2}\left[kH_1^*\frac{\dot{h}}{U_\infty} + kH_2^*\frac{b\dot{\alpha}}{U_\infty} + k^2H_3^*\alpha\right], \tag{4}$$

$$M = \frac{\rho U_\infty^2(2b)^2}{2}\left[kA_1^*\frac{\dot{h}}{U_\infty} + kA_2^*\frac{b\dot{\alpha}}{U_\infty} + k^2A_3^*\alpha\right], \tag{5}$$

where $k = \frac{\omega b}{U_\infty}$ is the reduced frequency of the motion, the angular frequency is $\omega = 2\pi f$; and f is the frequency of vibration. The aerodynamic lift and torque forces are the variables L and M; ρ is the density of the fluid; $b = \frac{B}{2}$ is the value corresponding to half chord length of the airfoil; h and $\dot{h}$ are the vertical motion of the airfoil and its time derivative; α and $\dot{\alpha}$ are the angular motion of the airfoil and its time derivative. The flutter derivatives are represented by A_j^* and H_j^* ($j = 1, 2, 3$), and they are functions of the reduced frequency k. Another important dimensionless parameter to be used is the reduced velocity, $U^* = \frac{U_\infty}{fb}$.

To find the flutter derivatives, purely vertical displacement must be applied first in order to obtain the lift and torque. Then, using Fourier transform, it is possible to extract their sinusoidal and cosinusoidal phases for each reduced frequency. The same procedure must be done by subjecting the body to a purely angular displacement. The expressions in eq. (6) have the functions for the vertical displacement $h(t)$ and for the angular oscillation $\alpha(t)$, respectively.

$$h(t) = h_0\sin(\omega t), \qquad \alpha(t) = \alpha_0\sin(\omega t). \tag{6}$$

With the forced vertical displacement represented by eq. (6) and according to eq. (4) and eq. (5), result

$$\frac{L(t)}{k^2 h_0 \rho U_\infty^2} = \left[H_1^* \cos(\omega t)\right], \tag{7}$$

$$\frac{M(t)}{k^2 h_0 \rho U_\infty^2 2b} = \left[A_1^* \cos(\omega t)\right]. \tag{8}$$

Note, by the expressions 7 and 8, that the coefficients H_1^* and A_1^* are obtained from the cosinusoidal components of the lift and the torque, respectively. Through the forced angular motion of eq. (6), applied to eq. (4) and eq. (5), it leads to

$$\frac{L(t)}{k^2 \alpha_0 \rho U_\infty^2 b} = \left[H_2^* \cos(\omega t) + H_3^* \sin(\omega t)\right], \tag{9}$$

$$\frac{M(t)}{k^2 \alpha_0 \rho U_\infty^2 2b^2} = \left[A_2^* \cos(\omega t) + A_3^* \sin(\omega t)\right]. \tag{10}$$

Therefore, the values of H_3^* and A_3^* are found from the sine phase of the lift and moment. The other coefficients are obtained with the cosine phases of these forces.

2.3 Numerical techniques

In the simulations, the OpenFOAM fluid dynamics program(*Open source Field Operation And Manipulation*) developed in C ++ language was used. The code is released with free and open-source status by GNU General Public License [5].

The equations were discretized using the finite volume method. The gradients were solved with centered schemes and second-order linear interpolation. The second-order linear upwind scheme was used for convective terms.

In the static analyzes, the SIMPLE (Semi Implicit Methods Pressure Linked Equations) technique was used for the pressure-velocity coupling, and the simulations were carried out in a steady-state with a dimensionless time step of 10^{-3}. In the oscillatory analyzes, the PIMPLE (Pressure Implicit with Splitting of Operators combined with SIMPLE) technique was used in a transient-state with an implicit scheme for advancing the time step. An adjustment of the automatic time steps was allowed as long as it does not violate a certain Courant number in the order of 0.9.

For flutter analysis, mesh motion is an important factor in the interaction between the fluid and the structure. As the prescribed motion of the body occurs, the mesh must somehow adapt to the position where the body is. To make the mesh movement, it is proposed to use an algorithm that solves the equations of motion of the mesh using the Laplace equation, where the boundary conditions must meet the kinematic conditions imposed by the prescribed displacements of the body. The nodes on the body surface have the displacements and velocities prescribed by the movement of the body, and the nodes on a predefined boundary have zero displacements and velocities. The spacing between the nodes is changed by lengthening or shortening smoothly, thus portraying the movement.

3 Numerical examples

This section presents the computational domain and boundary conditions. In the sequence, two numerical examples are presented. The first example is a static study of the flow around the NACA0012 airfoil, changing the angle of attack. The second study aims to obtain the flutter derivatives through forced vibrations, and the flutter theory described in Section2.2. For this purpose, body displacement and mesh movement algorithms described in Section 2.3 were used. A preliminary example for the study of mesh and the use of body motion algorithms is presented.

From this section on, the results found for this paper will be presented as "*Lucinda, 2020*".

3.1 Computational domain and boundary conditions

In any simulation, it is necessary to define a computational domain. For the proposed problems, a two-dimensional domain with its boundary conditions was used, as seen in the Fig. 1. The O point of the leading edge of a NACA 0012 geometry is defined as the origin coordinate, constructed using 80 nodal points and with a unitary B chord (see Fig. 2). The domain has 100 chord length units from the leading edge and a total height of 40 chord length units. The semi-circumference has a center at the origin and a radius of 20 units of chord length.

The domain boundaries for the application of boundary conditions are named: Top for the top face of the domain, $Bottom$ the bottom, $Inlet$ on the left, $Outlet$ on the right, and those that define the airfoil as $Wall$.

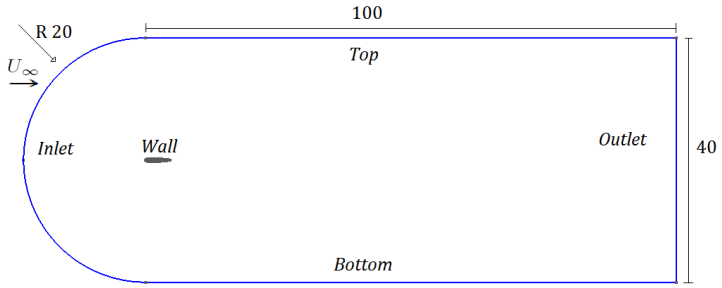

Figure 1. Fluid domain and boundary conditions

At the boundaries *Inlet, Top* and *Bottom*, uniform flow with unit velocity and zero pressure gradient were assumed. In *Outlet*, the zero pressure and zero velocity gradient condition were applied. On the airfoil walls *Wall*, the non-slip condition, and the zero pressure gradient were applied.

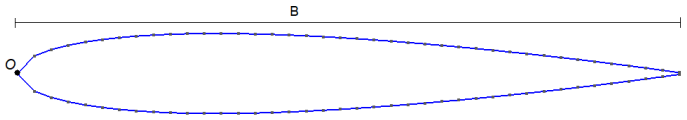

Figure 2. NACA 0012 airfoil defined with 80 points

3.2 First example - static analysis with the angle of attack variation

First, simulations were made for a static approach to the airfoil. The averages of the lift coefficients (Cl) and drag (Cd) were obtained by fixing the airfoil and submitting it to an incompressible and turbulent flow with ($Re = 7 \times 10^5$), for different angles of attack. A $k - \omega$ SST turbulence model with $I = 1\%$ and $L = 1$ was used.

For the simulations in this section, the domain presented in Section 3.1 was used. As it is turbulent flow, further refinement was necessary for the region close to the airfoil. An unstructured mesh with 3300 elements around the airfoil, 128120 nodes in every domain, and 124707 total triangular elements was used.

The calculated coefficients are presented in Fig. 3, where they are compared with the curves obtained from experimental results, found in Miley [7] and Sheldahl and Klimas [8]. The results are satisfactory, validating the proposed CFD model to obtain the aerodynamic coefficients. It was observed that, close to the stall region, characterized by the loss of airfoil lift, there are the greatest differences in results. For simulations with high angles of attack, it is recommended to use techniques that incorporate transient effects.

3.3 Second example - estimation of the flutter derivatives

Preliminary example

In order to choose the mesh to be used to obtain the flutter derivatives and perform the validation of the numerical techniques used for the mesh displacement, preliminary tests were conducted.

It is proposed to simulate a laminar flow to a Reynolds number of 3000 during 150 steps of time in the domain

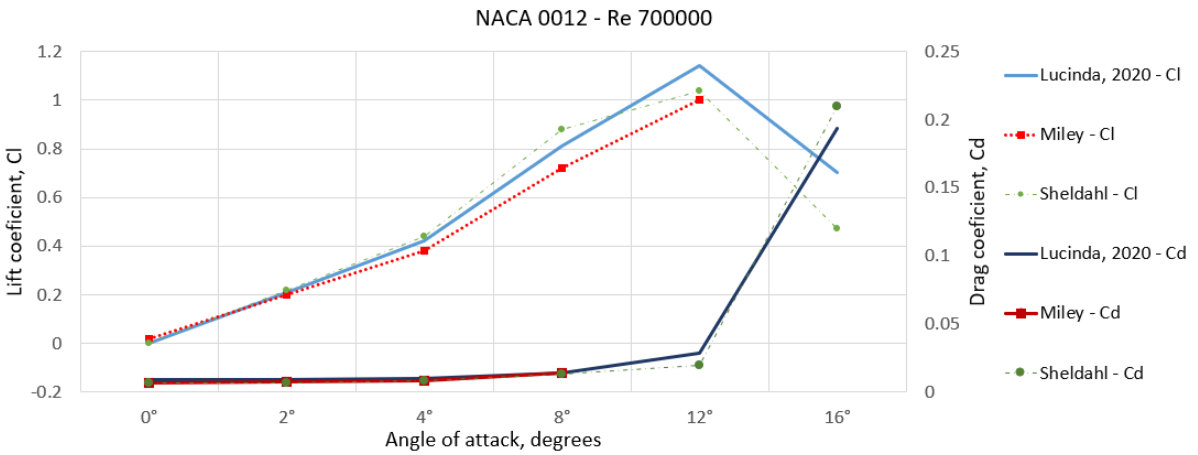

Figure 3. Aerodynamic lift and drag coefficients for different angles of attack in a NACA 0012 submitted to a Reynolds number equal 700000 .

presented in Section 3.1. The airfoil is under a forced rotation around its first third of string, with an angle of attack known through the equation eq. (11).

$$\alpha(t) = \alpha_0 - \overline{\alpha} \cdot \sin(2\pi t), \tag{11}$$

where the initial angle of attack is $\alpha_0 = 30°$, and the amplitude of motion is given by $\overline{\alpha} = 7°$. The PIMPLE scheme was used for decoupling pressure and velocity.

For the examples in this section, the use of the PIMPLE technique was mandatory, since it is the algorithm that must be used when the mesh moves. However, the use of the mesh of the example in Section 3.3 with the PIMPLE technique demanded a high computational cost. In order to reduce the computational cost, three new meshes with triangular elements were proposed, wherein each mesh 80 elements were conserved around the airfoil. The first mesh had a total of 80 elements in its horizontal (at the *Top* and *Bottom*), and in the vertical (in *Outlet*) a total of 50 elements. The second mesh had in its domain 100 elements in the horizontal and its borders and 50 elements in the vertical border *Outlet*. The third mesh, this more refined, had 100 elements at the *Top* and *Bottom* borders and 100 elements *Outlet*. The Table 1 shows the characteristics of these new meshes.

The aerodynamic forces obtained for each mesh are presented in Table 1. As the results found were similar, it was decided to use the mesh where the domain box has 100×50 elements. This mesh is shown in Fig. 4.It was observed that the algorithm used for the mesh and body motion behaved as expected, being used in the subsequent simulations.

Table 1. Mesh test

Elements (horizontal $\times$ vertical)	Number of nodes / elements	Lift (L)	Torque (M)
80×50	25324 / 24975	1.1505	0.6326
100×50	31784 / 31395	1.1816	0.6716
100×100	33562 / 33123	1.1842	0.6604

Estimation of flutter derivatives

The values of the flutter derivatives for NACA 0012 were obtained considering a fluid with dimensionless incidence velocity $U_\infty = 1$ and Reynolds number (Re) of 800. The pressure and velocity boundary conditions were the same as those presented in the Section 3.1.

Two different situations were performed, one subjecting the airfoil to pure vertical displacement $h(t)$ and the other to pure angular displacement $\alpha(t)$. In the middle of the airfoil chord, the displacements prescribed by the equations eq. (6) were applied, adopting $h_0 = 0.05b$ and $\alpha_0 = 2^o$.

Simulations were made for each reduced velocity U^*, obtaining the time history of the aerodynamic lift and torque coefficients in the middle of the airfoil chord. Through Fourier transforms, each flutter derivatives was

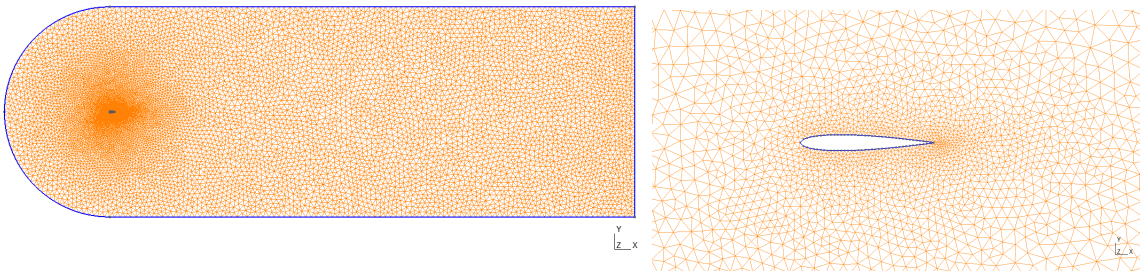

Figure 4. Mesh used in the domain on the left, refinement around the airfoil on the right.

extracted. The values of the flutter derivatives found are organized in Fig. 5. They are compared with the results obtained by Le Maıtre et al. [1], which adopted a numerical based on a streamfunction/velovity formulation in relative frame attached to the airfoils formulation.

The values of the parameters H_1^* and A_1^* has proximity to the reference values. The same is observed for H_3^* and A_3^*, being a good approximation and presenting a similar curve trend. The curves have greater differences for higher reduced velocities. For H_1^*, A_1^*, H_3^* and A_3^*, values were found, in module, lower than those found in Le Maıtre et al. [1]. These are values consistent with the theory.

For the H_2^* coefficients, a difference in the results is observed. However, there is a similarity in the behavior of the curve. The experiment proposed by Le Maıtre et al. [1] mentioned the difference between the results found for H_2^*, considering it far from the theoretical values. There are also differences in the results of A_2^*. The behavior of the curve is not similar to the reference curve.

In order to improve the H_2^* and A_2^* results, a refined mesh was propossed for the reduced velocity of 16. The mesh was refined using a total of 400 elements around the airfoil, and 100×50 was kept in the domain box. In total, this new mesh has 37494 elements. The results were plotted together in Fig. 5 with the title "Refinement". It is observed that, despite the greater refinement in the region close to the airfoil, there were no significant changes that justified the use of more elements in the mesh.

The proposed model performed a satisfactory response when compared to the reference values, despite certain differences. The parameters used, such as mesh size, mesh motion model, and CFD model, were sufficient to guarantee good results, requiring a low computational cost.

4 Conclusions

The present work had as main objective the application of CFD to reproduce the phenomena of stall and flutter in a symmetrical NACA 0012.

For the first case, a numerical model was proposed for the turbulent flow solution in steady-state using the k ω SST turbulence model. A good correlation between the obtained and the experimental results was observed.

A model for the numerical solution to extract the flutter derivatives was also presented. It was necessary to implement a mesh and control it to solve the Navier-Stokes equations. In this paper, the simulations were performed by applying known forced displacements to obtain the aerodynamic and flutter derivatives. The results found were compared with those already found in the literature. In general, a good approximation was observed for the reference values in the reduced velocity lower than 12. Similar behavior of curves and good values were found for both purely vertical and rotational movements, except for the H_2^* and A_2^* flutter derivatives.

In general, the present work presented expected results, thus validating the formulation used. The proposed method, therefore, can be used for future work and new profiles, such as structures like bridges.

Acknowledgements. The authors would like to thank to the Post Graduate Program in Civil Engineering (PEC), to the Federal University of Juiz de Fora (UFJF), and to the Coordenação de Aperfeiçoamento de Pessoal de Nível Superior (Capes) for the financial support.

Authorship statement. The authors hereby confirm that they are the sole liable persons responsible for the authorship of this work, and that all material that has been herein included as part of the present paper is either the property (and authorship) of the authors, or has the permission of the owners to be included here.

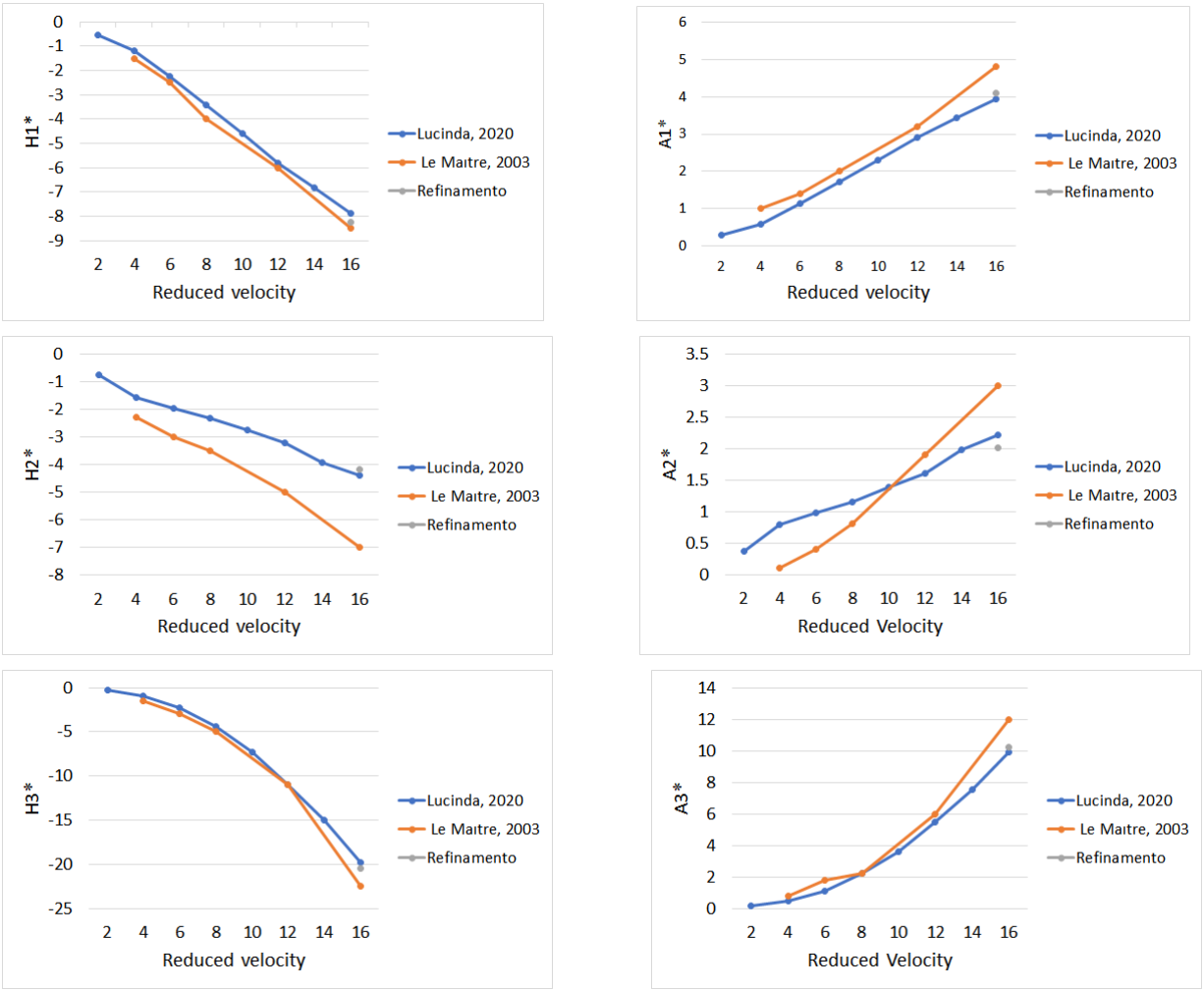

Figure 5. Flutter derivatives found for a NACA 0012 airfoil. Re = 800.

References

[1] Le Maitre, O., Scanlan, R., & Knio, O., 2003. Estimation of the flutter derivatives of an naca airfoil by means of navier–stokes simulation. *Journal of Fluids and Structures*, vol. 17, n. 1, pp. 1–28.

[2] Blevins, R. D., 2001. *Flow Induced Vibration*. Florida, USA.

[3] Dowell, E. H., Curtiss, H. C., Scanlan, R. H., & Sisto, F., 1989. *A modern course in aeroelasticity*, volume 3. Springer.

[4] Menter, F., 1993. Zonal two equation kw turbulence models for aerodynamic flows. In *23rd fluid dynamics, plasmadynamics, and lasers conference*, pp. 2906.

[5] Greenshields, C., 2019. The openfoam foundation user guide 7.0. *The OpenFOAM Foundation Ltd: London, United Kingdom, 10th July*.

[6] Scanlan, R. & Tomko, J., 1971. Airfoil and bridge deck aerodynamic parameters. *J. Eng. Mech*, vol. 97, n. 6, pp. 1171–1737.

[7] Miley, S. J., 1982. Catalog of low-reynolds-number airfoil data for wind-turbine applications. Technical report, Rockwell International Corp., Golden, CO (USA). Rocky Flats Plant; Texas A ....

[8] Sheldahl, R. E. & Klimas, P. C., 1981. Aerodynamic characteristics of seven symmetrical airfoil sections through 180-degree angle of attack for use in aerodynamic analysis of vertical axis wind turbines. Technical report, Sandia National Labs., Albuquerque, NM (USA).